Characterization of Kir1.1 Channels with the Use of a Radiolabeled Derivative of Tertiapin

John P. Felix,[‡,§] Jessica Liu,[‡,§] William A. Schmalhofer,[‡,§] Timothy Bailey,[‡,§] Maria A. Bednarek,[||] Stephanie Kinkel,[‡] Adam B. Weinglass,[‡] Martin Kohler,[‡] Gregory J. Kaczorowski,[‡] Birgit T. Priest,[‡] and Maria L. Garcia*[,‡]

Department of Ion Channels, and Medicinal Chemistry, Merck Research Laboratories, Post Office Box 2000, Rahway, New Jersey 07065

Received March 14, 2006; Revised Manuscript Received May 25, 2006

ABSTRACT: Inward rectifier potassium channels (Kir) play critical roles in cell physiology. Despite representing the simplest tetrameric potassium channel structures, the pharmacology of this channel family remains largely undeveloped. In this respect, tertiapin (TPN), a 21 amino acid peptide isolated from bee venom, has been reported to inhibit Kir1.1 and Kir3.1/3.4 channels with high affinity by binding to the M1−M2 linker region of these channels. The features of the peptide−channel interaction have been explored electrophysiologically, and these studies have identified ways by which to alter the composition of the peptide without affecting its biological activity. In the present study, the TPN derivative, TPN-Y1/K12/Q13, has been synthesized and radiolabeled to high specific activity with ^{125}I. TPN-Y1/K12/Q13 and mono-iodo-TPN-Y1/K12/Q13 ([^{127}I]TPN-Y1/K12/Q13) inhibit with high affinity rat but not human Kir1.1 channels stably expressed in HEK293 cells. [^{125}I]TPN-Y1/K12/Q13 binds in a saturable, time-dependent, and reversible manner to HEK293 cells expressing rat Kir1.1, as well as to membranes derived from these cells, and the pharmacology of the binding reaction is consistent with peptide binding to Kir1.1 channels. Studies using chimeric channels indicate that the differences in TPN sensitivity between rat and human Kir1.1 channels are due to the presence of two nonconserved residues within the M1−M2 linker region. When these results are taken together, they demonstrate that [^{125}I]TPN-Y1/K12/Q13 represents the first high specific activity radioligand for studying rat Kir1.1 channels and suggest its utility for identifying other Kir channel modulators.

Potassium channels regulate many critical cellular functions such as the electrical pattern of neurons, muscle contraction, hormone and neurotransmitter release, electrolyte movement, and cell proliferation (*1*). The large family of potassium channels contains, as a common structural feature, two transmembrane domains connected by a pore loop, the M1−M2 linker, where the potassium selectivity sequence resides. Four of these subunits assemble to form a functional tetrameric channel. Other structurally distinct domains can associate with the pore domain to yield channels that gate in response to different stimuli. The high-resolution X-ray structure of potassium channels has provided detailed information concerning the molecular mechanisms involved in ion permeation (*2*, *3*).

Inward rectifier potassium channels (Kir)[1] are the prototype of a minimum potassium channel structure in that they only consist of two transmembrane segments and a pore domain. Many residues in the N- and C-terminal regions of these proteins are important for the regulation of channel activity, as well as for their trafficking and interaction with other subunits. Inward rectification, defined as the capacity to carry more current in the inward than in the outward direction, is due to the voltage-dependent block of the channel by intracellular cations such as Mg^{2+} and polyamines (*4*, *5*). The molecular basis for inward rectification is well-understood from functional studies as well as from the high-resolution X-ray structure of the bacterial homologue of Kir1.1 (*6*, *7*).

The functional importance of inward rectifier potassium channels is highlighted by the fact that mutations in the genes encoding these proteins result in neuronal degeneration (Kir3.2), cardiac arrhythmias (Kir2.1), defective renal salt absorption (Kir1.1), and defective insulin secretion from pancreatic β cells (Kir6.2) (*8*, *9*). Despite the prominent role that Kir channels play in cell physiology, the molecular pharmacology of these channels remains mostly undeveloped. The only high-affinity probe for some members of the Kir family is tertiapin (TPN), a 21 amino acid peptide isolated from bee venom (*10*). TPN blocks Kir1.1 and Kir3.1/3.4 channels with high affinity by binding to residues present in the external end of the ion-conduction pore of these channels through a reversible bimolecular reaction. Other

* To whom correspondence should be addressed. Telephone: (732) 594-7564. Fax: (732) 594-3925. E-mail: maria_garcia@merck.com.
[‡] Department of Ion Channels.
[§] These authors contributed equally to this work.
[||] Medicinal Chemistry.

[1] Abbreviations: Kir, inward rectifier potassium channel; TFA, trifluoroacetic acid; TPN, tertiapin; [^{125}I]-TPN-Y1/K12/Q13, mono-iodotyrosine-TPN-Y1/K12/Q13; K_d, equilibrium dissociation constant; K_i, equilibrium inhibition constant; k_1, association rate constant; k_{-1}, dissociation rate constant; MCDP, mast cell degranulating peptide; ChTX, charybdotoxin; IbTX, iberiotoxin; MgTX, margatoxin; DTX, dendrotoxin; ShK, *Stichodactyla helianthus* peptide.

10.1021/bi060509s CCC: $33.50
Published on Web 07/25/2006

Kir channels, such as Kir2.1, are insensitive to the peptide. The nuclear magnetic resonance (NMR) structure of TPN indicates a backbone consisting of a C-terminal α helix (residues 12−19) and a more extended conformation at the N terminus, with both parts being held together by two pairs of disulfide bonds. Methionine at position 13 can undergo air oxidation, causing a loss in the channel-blocking affinity of the peptide, but glutamine substitution yields a stable and fully functional peptide (*11*). In addition, the presence of histidine at position 12 causes the block of the channel to be pH-dependent, with deprotonation of the histidine residue causing a large decrease in the binding energy of the peptide. Substitution of lysine at this position is tolerated and eliminates the pH dependence of the channel block (*12*). Extended mutagenesis studies support the idea that TPN binds to the outer vestibule of the Kir channel through its α helix and that the extended N-terminal region projects out of the vestibule into the extracellular medium (*13*). These data suggest that the N terminus represents a favorable region for incorporation of labels and development of a probe with which to study the interaction of TPN with Kir channels.

In the present study, TPN-Y1/K12/Q13 has been prepared and radiolabeled to high specific activity with ^{125}I. Both parent and mono-iodo-derivative peptides inhibit rat Kir1.1 channels with high affinity. Specific and saturable binding of mono-iodo-TPN-Y1/K12/Q13 ([^{125}I]TPN-Y1/K12/Q13) has been observed to cell-surface-expressed channels in HEK293 cells stably transfected with rat Kir1.1 and to membranes derived from these cells. High-affinity binding of [^{125}I]TPN-Y1/K12/Q13 was not detected to human Kir1.1 channels, consistent with the reduced sensitivity of these channels to TPN peptides. Chimeric channels of human and rat Kir1.1-containing residues from the M1−M2 linker regions provide insights into the molecular determinants of human Kir1.1 that are responsible for its reduced sensitivity to TPN. When these data are taken together, they indicate that [^{125}I]TPN-Y1/K12/Q13 represents a novel, useful probe for studying Kir1.1 channels and for developing their pharmacology.

EXPERIMENTAL PROCEDURES

Materials. Restriction enzymes and the pCI-neo vector were obtained from Promega. The pcDNA5/FRT/TOPO-TA vector and all tissue culture media were from Invitrogen Corp. (Carlsbad, CA). Human and rat kidney cDNA and Advantage2 DNA polymerase were purchased from Clontech Biosciences (Palo Alto, CA). QuickchangeII site-directed mutagenesis kit was from Stratagene (La Jolla, CA). Dye terminator sequence reactions were performed with the ABI BigDye3.1 sequencing kit and analyzed with an ABI3100 genetic analyzer, both from Applied Biosystems (Foster City, CA). HEK293 cell lines were from American Type Culture Collection (Manassas, VA), and TsA-201 cells were a gift of Dr. Robert DuBridge. The IODO-GEN reagent was from Pierce, and Na[^{125}I] was from New England Nuclear Corp. Apamin, mast cell degranulating peptide (MCDP), charybdotoxin (ChTX), iberiotoxin (IbTX), *Stichodactyla helianthus* peptide (ShK), α-dendrotoxin (α-DTX), and δ-dendrotoxin (δ-DTX) were obtained from Peptides International; the FuGENE6 transfection reagent was from Roche; and the protease inhibitor cocktail was from Sigma. Margatoxin (MgTX), agitoxin1 (AgTX1), and agitoxin2 (AgTX2) were prepared as described (*14*). All other reagents were obtained from commercial sources and were of the highest purity commercially available.

Synthesis of TPN Peptides. Elongation of the peptide chains were performed on an ABI peptide synthesizer using supplier-provided protocols. The peptidic materials were cleaved from the resin with trifluoroacetic acid (TFA) containing anisole and mercaptoethanol and then air-oxidized in 10% NH_4OAc solution at pH 8.2−8.5 overnight. Preparative purification of the crude products was performed on a Waters Delta Prep 4000 system with a semipreparative C_{18} Vydac reverse-phase column, in a water−acetonitrile gradient system of 0−60% buffer B in 60 min (buffer A was 0.5% TFA in water, and buffer B was 0.5% TFA in acetonitrile). The chromatographically homogeneous, folded peptides were analyzed by electrospray mass spectrometry and reverse-phase high-pressure liquid chromatography (C_{18} Vydac analytical column, a gradient of 0−40% buffer B in 30 min of the above-described solvent system, with a 1.5 mL/min flow rate).

Iodination of TPN-Y1/K12/Q13. For iodination with either Na[^{125}I] or Na[^{127}I], 2.5 μg of IODO-GEN was dissolved in 50 μL of acetone in a 1 mL Wheaton v-vial. The solution was dried under argon to coat the walls of the vial with IODO-GEN (reaction vial). The reaction vial was rinsed twice with 200 μL of $NaPO_4$ at pH 8.0, and 15 μL of $NaPO_4$ at pH 8.0 was added to the vial, followed by the addition of 20 μL of TPN-Y1/K12/Q13 solution (0.64 mg/mL in 100 mM $NaPO_4$ at pH 8.0) and 14 μL of a solution containing either 5 mCi of Na[^{125}I] (2200 Ci/mmol) or 20 μg/mL Na[^{127}I] in 10 μM NaOH. After incubation at room temperature for 10 min, the sample was loaded onto a 300 Å pore-size C_{18} reverse-phase HPLC column (Vydac, 0.46 × 25 cm) that had been equilibrated with 10 mM TFA. Elution was achieved with a linear gradient of 30% acetonitrile in 10 mM TFA (0−35% at 2 min and 35−90% at 30 or 40 min) at a flow rate of 0.5 mL/min. Material eluting from the column was monitored by measuring the absorbance at 210 nm. Individual peaks were lyophilized dry and reconstituted in 100 mM NaCl, 20 mM Tris-HCl at pH 7.4 and 0.1% bovine serum albumin. Aliquots were frozen in liquid N_2 and stored at −70 °C. After the iodination of the peptide with Na[^{127}I], chromatographically homogeneous peaks corresponding to the parent and its iodinated derivatives were collected and analyzed by electrospray mass spectroscopy.

Channel Constructs. Kir1.1 cDNA was amplified by polymerase chain reaction (PCR) using rat or human kidney Quickclone cDNA as a template. Sequence-specific oligonucleotide primers (Table 1) to amplify the entire coding region of Kir1.1 were designed on the basis of the published nucleic acid sequence (rat Kir1.1 GenBank accession X72341 and human Kir1.1 GenBank accession NM_000220). The PCR reactions were performed with Advantage2 DNA polymerase with the following conditions: 1 min at 95 °C for 1 cycle and 15 s at 95 °C and 3 min at 68 °C for 35 cycles. A fragment of the expected size was amplified and subsequently cloned into the pcDNA5/FRT/TOPO-TA vector. The identity of the cDNA insert was verified by sequencing. For generation of stable cell lines, the insert was cloned as a *Mlu*I−*Not*I fragment into the pCIneo expression vector.

Table 1: Oligonucleotide Primers for Cloning and Mutagenesis of Rat and Human Kir1.1[a]

hKir1.1(A116D)-as	GGAGTGTGATTG**T**CAGAAGGATGGAATTC
hKir1.1(A116D)-s	GAATTCCATCCTTCTG**A**CAATCACACTCC
hKir1.1(L128M)-as	CAGAAAAGCTGAGGTCA**T**GCCATTAATATTCTC
hKir1.1(L128M)-s	GAGAATATTAATGGC**A**TGACCTCAGCTTTTCTG
hKir1.1(C148F)-as	ACACTGTTCTGTCACA**A**ACCTGAATCCATATCC
hKir1.1(C148F)-s	GGATATGGATTCAGGT**T**TGTGACAGAACAGTGT
hKir1.1(H113Y,S115P,A116D,H118R)-as	CACACAGGGAGTG**C**GATTG**T**CAG**G**AGGATA**G**AATTCCGGGAG
hKir1.1(H113Y,S115P,A116D,H118R)-s	CTCCCGGAATTC**T**ATCCT**C**CTG**A**CAATC**G**CACTCCCTGTGTG
ratKir1.1-(*Not*I)-as	gcatgcggccgc**TTA**CATCTGGGTGTCGTCCGTTTCATCAAC
ratKir1.1-(*Mlu*I)-s	gcatacgcgttaaacc**ATG**GGCGCTTCGGAACGGAGTGTG
human Kir1.1-(*Not*I)-as	gatgcggccgc**TTA**CATTTTGGTGTCATCTGTTTCATTGAC
human Kir1.1(*Mlu*I)-s	tacacgcgttaaacc**ATG**AATGCTTCCAGTCGGAATGTGT

[a] The -s suffix denotes a primer in the sense orientation, and the -as suffix denotes a primer in the antisense orientation. All oligonucleotide primers are written in the 5′ → 3′ direction.

Preparation of Cells Stably Expressing Rat and Human Kir1.1. Rat or human Kir1.1 pCIneo expression plasmids were transfected into HEK293 cells with FuGENE6. A stable pool of HEK293 cells expressing rat or human Kir1.1 was prepared by neomycin selection (750 μg/mL). Stable pools were analyzed for functional expression of Kir1.1 using a membrane potential, fluorescence resonance energy-transfer-based assay as described (*15*). Individual stable cell lines were generated by limited dilution under continuous selection with neomycin (500 μg/mL). Cell lines were selected on the basis of the signal intensity in the functional fluorescent assay.

Pore Mutant Constructs of Human Kir1.1. Site-directed mutagenesis was performed with the QuickchangeII kit. The oligonucleotides used for mutagenesis are listed in Table 1. Starting with a plasmid carrying the human Kir1.1wt cDNA, the primer pair hKir1.1(H113Y, S115P, A116D, H118R)-s and -as was used to introduce changes at the indicated positions. This mutant Kir1.1 cDNA was used to create hKir1.1-mut1, -mut2, and -mut5. In addition, the primer pair hKir1.1(C148F)-s and -as was used to generate hKir1.1-mut3 from hKir1.1wt cDNA, which subsequently served as a basis to construct hKir1.1-mut4 and -mut8. To generate hKir1.1-mut6 and -mut7, hKir1.1wt cDNA and appropriate primer pairs were used. For all mutants, the entire insert was sequenced to exclude secondary amino acid changes. The pore sequence for these mutants is depicted in Figure 5.

Transfection of TsA-201 Cells and Membrane Preparation. Procedures for handling TsA-201 cells and their transfection with FuGENE6 have been previously described (*16*). For the preparation of membrane vesicles, cells were pelleted and homogenized in 250 mM sucrose and 25 mM Hepes-NaOH at pH 7.4, supplemented with 1 μL/mL of protease inhibitor cocktail. Homogenates were centrifuged at 1000*g* for 10 min, and the supernatant was collected by centrifugation at 100000*g* for 45 min. The pellet was resuspended in homogenization buffer, layered on top of a discontinuous 20−40% sucrose gradient, and centrifuged at 100000*g* for 1 h. Material at the 40% sucrose interface was collected, diluted with 100 mM NaCl and 20 mM Hepes-NaOH at pH 7.4, and subjected to centrifugation at 100000*g* for 45 min. Membrane pellets were resuspended in 100 mM NaCl and 20 mM Tris-HCl at pH 7.4, and aliquots were quickly frozen in liquid N_2 and stored at −80 °C. For electrophysiological recordings, 35 mm polystyrene Petri dishes containing 3 × 3 mm poly-D-lysine-coated glass chips were seeded 24 h after transfection.

^{125}I-TPN-Y1/K12/Q13 Binding. For binding to cells, 96-well poly-D-lysine-coated plates were seeded at a density of 75 000 cells per well and cells were allowed to attach for approximately 18 h at 37 °C. [^{125}I]-TPN-Y1/K12/Q13 was added to wells, and incubation took place under normal growth conditions. For saturation experiments, cells were incubated with increasing concentrations of [^{125}I]-TPN-Y1/K12/Q13 for 8 h and quadruplicate samples were averaged for each experimental point. Competition binding experiments were carried out in the absence or presence of an increasing concentration of test peptide. To determine the kinetics of ligand association, cells were incubated with [^{125}I]-TPN-Y1/K12/Q13 for different periods of time. Dissociation kinetics were initiated either by the addition of 100 nM TPN-Y1/K12/Q13 or by washing the wells 4 times with media and incubating for different periods of time. Nonspecific binding was defined as binding in the presence of 100 nM TPN-Y1/K12/Q13. At the end of the incubation, cells were washed twice with 200 μL of Dulbecco's phosphate-buffered saline to separate bound from free ligand, and radioactivity associated with cells was determined using a γ counter. Unless otherwise stated, the interaction of [^{125}I]-TPN-Y1/K12/Q13 with membranes was determined in a medium consisting of either 50 or 100 mM KCl, with 20 mM Tris-HCl at pH 7.4 and 0.1% bovine serum albumin. Incubations were carried out at room temperature, for at least 5 h in a total volume of 2 mL (50 mM KCl) or 1 mL (100 mM KCl). For saturation experiments, membranes were incubated with increasing concentrations of [^{125}I]-TPN-Y1/K12/Q13. Competition experiments were carried out with [^{125}I]-TPN-Y1/K12/Q13 in the absence or presence of an increasing concentration of the test compound. To determine the kinetics of ligand association, membranes in 50 mM KCl were incubated with [^{125}I]-TPN-Y1/K12/Q13 for different periods of time. Dissociation kinetics were initiated either by the addition of 1 nM TPN-Y1/K12/Q13 or by 50-fold dilution and incubating for different periods of time at room temperature. Nonspecific binding was defined as binding in the presence of 1−10 nM TPN-Y1/K12/Q13. The separation of bound from free ligand was achieved by diluting samples with 4 mL of ice-cold buffer, consisting of 100 mM NaCl, 20 mM Tris-HCl at pH 7.4, and 0.1% bovine serum albumin, and filtering through GF/C glass-fiber filters presoaked in 0.5% polyethylenimine. Filters were rinsed twice with 4 mL of ice-cold buffer. Data from saturation, competition, and ligand dissociation experiments were analyzed as described (*17*, *18*). The association rate constant, k_1, was determined

by employing both the pseudo-first-order rate equation $k_1 = k_{obs}([LR]_e/([L][LR]_{max}))$ or the second-order rate equation $k_1 = [1/([L] - [LR]_{max})][([L] - [LR]_t)/([LR]_{max} - [LR]_t)]$, where $[LR]_e$ is the concentration of the complex at equilibrium, [L] is the concentration of ligand, $[LR]_{max}$ is the total receptor concentration, k_{obs} is the slope of the pseudo-first-order plot, $\ln([LR]_e/([LR]_e - [LR]_t))$ versus time, and $[LR]_t$ is the receptor−ligand complex at one given time point *t*. [^{125}I]-TPN-Y1/K12/Q13 was determined to exhibit catastrophic decay after comparing the behavior of the radiolabeled peptide that had undergone five half-life decays with the newly radiolabeled peptide in saturation binding studies.

Electrophysiological Recordings. The block of Kir1.1 by TPN analogues was examined by whole-cell voltage clamp (*19*) using an EPC-9 amplifier and Pulse software (HEKA Electronics, Lamprecht, Germany). Experiments were performed at room temperature. Electrodes were fire-polished to resistances of 2−4 MΩ. Voltage errors were minimized by series resistance compensation, and the capacitance artifact was canceled using the built-in circuitry of EPC-9. Data were acquired at 10 kHz and filtered at 2.9 kHz. The bath solution consisted of 100 mM NaCl, 60 mM KCl, 2.7 mM $CaCl_2$, 0.5 mM $MgCl_2$, and 5 mM Na-HEPES at pH 7.4. To assess the quality of the recording and the contribution of Kir1.1 to the current at negative holding potentials, a second bath solution containing a low concentration of K^+ (150 mM NaCl, 10 mM KCl, 2.7 mM $CaCl_2$, 0.5 mM $MgCl_2$, and 5 mM Na-HEPES at pH 7.4) was used at the beginning of each recording and the shift in the current reversal between the bath solutions containing 60 and 10 mM K^+ was examined. The calculated shift in reversal potential for a K^+ selective current under these conditions was 45 mV, and a shift of at least 40 mV was considered acceptable. The internal (pipet) solution contained 130 mM KCl, 5 mM NaCl, 2 mM $MgCl_2$, 5 mM EGTA, 0.2 mM MgATP, and 5 mM Na-HEPES at pH 7.4. Kir1.1 currents were measured by applying 100 ms voltage ramps from −100 to +100 mV at 10 s intervals and averaging the current evoked at membrane potentials between −100 and −98 mV. For TPN-Y1/K12/Q13, IC_{50} (1.16 ± 0.22 nM) and Hill coefficient (1.4 ± 0.2) values were also determined during voltage steps to −100 mV. These values are not significantly different from those determined using voltage ramps. To avoid K^+ accumulation, cells were held at −30 mV throughout the experiment. Data are presented as mean ± standard error of the mean.

RESULTS

Synthesis and Biological Activity of TPN-Y1/K12/Q13. A large body of experimental evidence suggests that TPN inhibits Kir1.1 and Kir3.1/3.4 channels by binding in a 1:1 stoichiometry to residues located in the M1−M2 linker and physically occluding the ion-conduction pathway (*13*). The α helix at the C-terminal region of TPN appears to be involved in close interactions with specific channel residues, whereas the N-terminal half acquires a more extended conformation and is predicted to face the extracellular medium. A double TPN mutant, TPN-K12/Q13, has been reported to retain similar biological activity as the parent peptide but lacks two properties of TPN: (1) pH dependence of the block because of the presence of histidine at position 12 and (2) the lack of stability because of the oxidation of methionine 13 (*12*). Because TPN-K12/Q13 does not contain residues for covalent incorporation of iodine and to develop a probe that could be radiolabeled to high specific activity for use in radioligand-binding studies, tyrosine was substituted at position 1 in TPN-K12/Q13. TPN-Y1/K12/Q13 was synthesized by solid-phase synthesis, folded, and purified. The properties of TPN-Y1/K12/Q13 were evaluated in electrophysiological recordings of rat Kir1.1 channels stably expressed in HEK293 cells. Because Kir1.1 channels are open at all membrane potentials, nonselective leak currents cannot be easily subtracted. Therefore, whole-cell currents were recorded in 10 and 60 mM K^+ at the start of an experiment, and the shift in the reversal potential was used to assess the quality of the recording and the contribution of nonselective leak currents (Figure 1A). Voltage ramps from −100 to +100 mV were then used to examine Kir1.1 currents under control conditions and in the presence of increasing concentrations of TPN-Y1/K12/Q13 (Figure 1B). The average current amplitude at voltages between −100 and −98 mV was used to monitor the time-dependent block of Kir1.1 by TPN-Y1/K12/Q13 (Figure 1C). The average ($n = 4$) fractional current blocked was best-fit by the Hill equation with an IC_{50} of 1.02 nM and a Hill coefficient of 1.7 (Figure 1D). Average IC_{50} and Hill coefficient values from the individual fits were 1.15 ± 0.22 nM and 1.3 ± 0.3 ($n = 4$), respectively. Similar to previously published data (*12*), TPN-K12/Q13 was found to be a potent blocker of rat Kir1.1 channels, blocking the inward current with an IC_{50} of 0.60 ± 0.10 nM and Hill coefficient of 0.69 ± 0.06 ($n = 3$; data not shown). The difference in IC_{50} values between TPN-Y1/K12/Q13 and TPN-K12/Q13 was not significant ($p = 0.11$). These data are consistent with the idea that the N-terminal extended region of the peptide does not make intimate contact with the channel and therefore represents a place for tolerated substitutions.

Chemical Modification of TPN-Y1/K12/Q13 by Iodination. To obtain a high specific activity ligand for Kir1.1 channels, TPN-Y1/K12/Q13 was reacted with Na[^{125}I], under the conditions described in the Experimental Procedures and resulting products were separated by C_{18} reverse-phase chromatography (Figure 2A). One reaction product was identified as the mono-iodo adduct of TPN-Y1/K12/Q13 on the basis of specific activity corresponding to the maximum theoretical value for incorporation of one iodine per peptide molecule. This peptide, [^{125}I]-TPN-Y1/K12/Q13, elutes from reverse-phase chromatography well-separated from native peptide and another peptide characterized as the di-iodo derivative of TPN-Y1/K12/Q13. To further confirm the identity of these peptides, TPN-Y1/K12/Q13 was iodinated under identical conditions with Na[^{127}I] and the resulting peptides were characterized by electrospray mass spectroscopy. The injection of 10 μL of the HPLC peak corresponding to unmodified TPN-Y1/K12/Q13 reveals the presence of triply (846.1^{3+}) and quadruply (634.3^{4+}) charged ions that reconstruct to yield a molecular weight of 2535.3 Da. Injection of the HPLC peak corresponding to mono-iodinated TPN-Y1/K12/Q13 reveals the presence of triply (888.0^{3+}) and quadruply (666.4^{4+}) charged ions that reconstruct to yield a molecular weight of 2661 Da.

The biological activity of [^{127}I]-TPN-Y1/K12/Q13 was determined in electrophysiological recordings of rat Kir1.1 channels. The mono-iodinated peptide inhibits rat Kir1.1 channels with IC_{50} values of 3.45 ± 0.69 nM and Hill

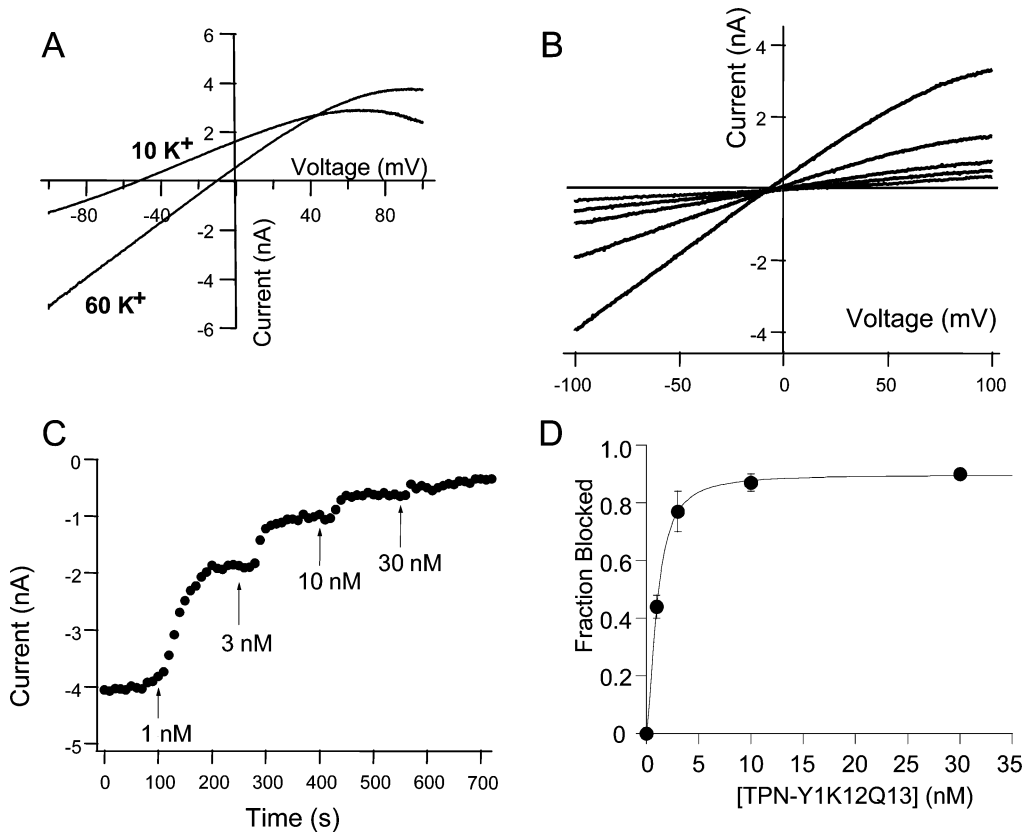

FIGURE 1: Inhibition of rat Kir1.1 channels by TPN-Y1/K12/Q13. Rat Kir1.1 channels stably expressed in HEK293 cells were examined by whole-cell voltage-clamp experiments as described under the Experimental Procedures. (A) Voltage ramps (from −100 to +100 mV in 1 s) in 10 and 60 mM external K^+ were used to assess the quality of the whole-cell recording. (B) Voltage ramps (from −100 to +100 mV in 0.1 s) in 60 mM external K^+ in the control and in the presence of 1, 3, 10, and 30 nM TPN-Y1/K12/Q13. (C) Inward current at voltages between −100 and −98 mV, determined during 0.1 s voltage ramps, as a function of time in the control and in the presence of indicated concentrations of TPN-Y1/K12/Q13. (D) Average fraction blocked is plotted versus the TPN-Y1/K12/Q13 concentration. The data are presented as the average fraction blocked in four separate experiments, and error bars represent the standard error of the mean. The solid line is a fit of the Hill equation to the average data with an apparent IC_{50} of 1.02 nM and a slope of 1.7.

coefficient of 1.2 ± 0.2 ($n = 4$) (Figure 2B). Although the difference in IC_{50} values between [^{127}I]-TPN-Y1/K12/Q13 and TPN-Y1/K12/Q13 is significant ($p = 0.02$), the data suggest that the iodination reaction did not markedly affect the biological activity of TPN-Y1/K12/Q13.

Binding of [^{125}I]-TPN-Y1/K12/Q13 to Cell-Surface-Expressed Rat Kir1.1 Channels. To determine whether [^{125}I]-TPN-Y1/K12/Q13 can be used to characterize rat Kir1.1 channels, HEK293 cells stably expressing the channel were incubated with radiolabeled peptide in the absence or presence of an excess of unlabeled TPN-Y1/K12/Q13. Specific binding of [^{125}I]-TPN-Y1/K12/Q13 to cell-surface-expressed channels was observed in these cells, and as expected, binding was cell-concentration-dependent (data not shown). Specific binding of [^{125}I]-TPN-Y1/K12/Q13 was not observed to HEK293 that do not express rat Kir1.1 channels (data not shown). Incubation of [^{125}I]-TPN-Y1/K12/Q13 with HEK293 cells for up to 2 days at 37 °C did not alter the binding characteristics of the peptide to cells expressing rat Kir1.1 channels, suggesting that [^{125}I]-TPN-Y1/K12/Q13 is stable in the cell incubation media. To further characterize the binding reaction, poly-D-lysine-coated 96-wells plates were seeded with ~75 000 cells and incubated with increasing concentrations of [^{125}I]-TPN-Y1/K12/Q13 until equilibrium was achieved, in the absence or presence of 100 nM TPN-Y1/K12/Q13 (Figure 3A). Specific binding displayed a good signal-to-noise ratio and was a saturable function of the [^{125}I]-TPN-Y1/K12/Q13 concentration. As expected, the nonspecific binding component varied linearly with the [^{125}I]-TPN-Y1/K12/Q13 concentration. The equilibrium dissociation constant, K_d, calculated from these experiments was 0.57 ± 0.06 nM; Hill coefficients were 1.04 ± 0.11; and the maximum density of cell-surface channels, B_{max}, equaled 95 900 ± 7300 channels/cell ($n = 3$). The K_d value calculated from equilibrium binding studies was in close agreement with the IC_{50} value for the channel block determined in electrophysiological recordings. In agreement with the lower sensitivity of human Kir1.1 to TPN peptides (see below), binding of [^{125}I]-TPN-Y1/K12/Q13 was not observed to HEK293 cells stably transfected with this channel.

The kinetics of [^{125}I]-TPN-Y1/K12/Q13 binding have been measured to determine whether peptide association occurs through a simple bimolecular reaction. The data presented in Figure 3B illustrate that incubation of 0.07 or 0.5 nM [^{125}I]-TPN-Y1/K12/Q13 with HEK293 cells expressing rat Kir1.1 resulted in a time-dependent association of the peptide with cell-surface-expressed channels that reached equilibrium at ~5 h. The nonspecific binding component is time-independent and has been subtracted from the experimental data. A semi-logarithmic transformation of the data (inset of Figure 3B) yielded linear dependences, as expected for pseudo-first-order reactions, and the slopes of the lines give k_{obs} values of 0.76×10^{-2} and 2.12×10^{-2} min^{-1}, respectively. Average k_{obs} values calculated from these experiments are 1.16×10^{-2}

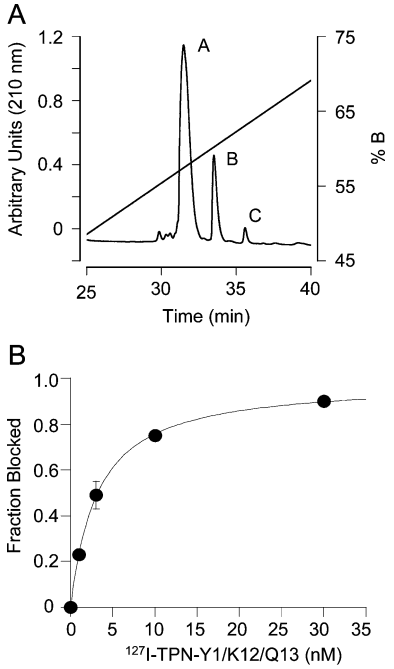

FIGURE 2: Iodination of TPN-Y1/K12/Q13. (A) HPLC separation of iodinated derivatives. TPN-Y1-K12/Q13 was subjected to iodination using the IODO-GEN method as described under the Experimental Procedures. The reaction mixture was loaded onto a HPLC C_{18} reverse-phase column equilibrated with 10 mM TFA, and elution was achieved with a linear gradient of 30% acetonitrile in 10 mM TFA (0−35% at 2 min and 35−90% at 30 min) at a flow rate of 0.5 mL/min. Material eluting from the column was monitored by measuring the absorbance at 210 nm. Peaks A, B, and C correspond to unmodified TPN-Y1/K12/Q13, mono-iodotyrosine-TPN-Y1/K12/Q13, and di-iodo-tyrosine-TPN-Y1/K12/Q13, respectively. (B) Inhibition of rat Kir1.1 by [^{127}I]-TPN-Y1/K12/Q13 as determined by whole-cell electrophysiology. Data are presented as the average fraction blocked in four separate experiments, and error bars represent the standard error of the mean. The solid line is a fit of the Hill equation to the average data with an apparent IC_{50} of 3.11 nM and a slope of 1.0.

$\pm$ 0.34 $\times$ 10^{-2} min^{-1} (n = 3) and 1.94 $\times$ 10^{-2} $\pm$ 0.25 $\times$ 10^{-2} min^{-1} (n = 2) for incubations at 0.07 and 0.5 nM [^{125}I]-TPN-Y1/K12/Q, respectively. The association rate constant, k_1, calculated as described under the Experimental Procedures, was 3.1 $\times$ 10^7 $\pm$ 0.7 $\times$ 10^7 M^{-1} min^{-1} (n = 5). Dissociation of cell-bound [^{125}I]-TPN-Y1/K12/Q13, initiated either by ligand dilution or by the addition of excess TPN-Y1/K12/Q13, followed a monoexponential decay with a $t_{1/2}$ of 72 min, corresponding to k_{-1} of 8.7 $\times$ 10^{-3} min^{-1} (Figure 3C). Average values from individual experiments give k_{-1} of 9.2 $\times$ 10^{-3} $\pm$ 1.2 $\times$ 10^{-3} min^{-1} (n = 3). The K_d calculated from these rate constants was 0.31 nM, a value that is similar to that determined under equilibrium binding conditions.

Binding of [^{125}I]-TPN-Y1/K12/Q13 to HEK293 cells expressing rat Kir1.1 was inhibited in a concentration-dependent manner by increasing concentrations of TPN-Q13, TPN-K12/Q13, or TPN-Y1/K12/Q13 (Figure 3D). K_i values, determined as described under the Experimental Procedures, are presented in Table 2 and display the expected rank order of potency for the interaction with the Kir1.1 channel. Other bee venom peptides that block Kir3.1/3.4 channels with low affinity (K_d > 1 μM), such as apamin and MCDP (*10*), had little (47% inhibition for MCDP, Figure 3D) or no effect (apamin, data not shown) on [^{125}I]-TPN-Y1-K12/Q13 binding to rat Kir1.1, when tested at concentrations up to 1 μM. Two other peptides, δ-DTX and Lq2, that have been reported to be weak inhibitors of rat Kir1.1 (*20*, *21*) inhibited the binding reaction by 12 and 33% at 1 and 3 μM (δ-DTX), respectively, and 18% at 1 μM (Lq2), whereas α-DTX had no effect up to 1 μM (Figure 3D). In addition, several peptide inhibitors of potassium channels that do not block rat Kir1.1 (*20*), such as ChTX, IbTX, MgTX, AgTX1, AgTX2, and ShK, had no effect on the binding reaction when tested at concentrations up to 1 μM (data not shown). These data, taken together, suggest that [^{125}I]-TPN-Y1/K12/Q13 represents a useful tool with which to investigate cell-surface-expressed rat Kir1.1 channels.

Binding of [^{125}I]-TPN-Y1/K12/Q13 to Membranes Derived from HEK293 Cells Expressing Rat Kir1.1 Channels. The interaction of [^{125}I]-TPN-Y1/K12/Q13 with rat Kir1.1 channels was also characterized using purified membranes prepared from HEK293 cells stably expressing rat Kir1.1. Unlike binding to intact cells where cell integrity is critical, membranes provide a system where experimental conditions, such as ionic composition, pH, and temperature, can be easily manipulated to enhance the strength of the peptide−channel interaction. Figure 4A presents data from experiments in which the binding of [^{125}I]-TPN-Y1/K12/Q13 to rat Kir1.1 HEK membranes was determined in the presence of different concentrations of KCl in the incubation medium. In the absence of KCl, specific binding of [^{125}I]-TPN-Y1/K12/Q13 was very low but increased as the concentration of KCl was raised to 31−56 mM and then decreased to become undetectable at concentrations above 250 mM KCl. Specific binding of [^{125}I]-TPN-Y1/K12/Q13 was not detected under any conditions to membranes prepared from HEK293 cells that do not express rat Kir1.1 channels. The dependence on potassium for high-affinity binding has been observed with other peptide inhibitors of potassium channels (*17*, *22*, *23*), and this effect most likely reflects the occupancy of potassium-binding sites in the selectivity filter conferring an appropriate architecture to the outer vestibule of the channel (*24*), because it cannot be mimicked by nonpermeant ions such as sodium (data not shown). On the other hand, the inhibitory effect of potassium observed at higher concentrations is most likely due to an ionic strength effect on binding because it also occurs in the presence of increasing concentrations of NaCl (data not shown).

Binding of [^{125}I]-TPN-Y1/K12/Q13 was further characterized at two different concentrations of KCl, 50 and 100 mM. When membranes were incubated with increasing concentrations of [^{125}I]-TPN-Y1/K12/Q13 until equilibrium was achieved, peptide association occurred in a concentration-dependent fashion under both experimental conditions (Figure 4B). Specific binding of [^{125}I]-TPN-Y1/K12/Q13 to rat Kir1.1 HEK membranes was saturable and could be fitted to a single-site model with a K_d of 1.01 $\pm$ 0.09 pM, a Hill coefficient of 1.03, and a B_{max} of 0.75 pmol/mg of protein (n = 3) for the 50 mM KCl experimental condition and a K_d of 8.85 $\pm$ 0.39 pM, a Hill coefficient of 0.97, and a B_{max} of 1.1 pmol/mg of protein (n = 3) for experiments carried out in 100 mM KCl.

The kinetics of [^{125}I]-TPN-Y1/K12/Q13 binding to membranes in the presence of 50 mM KCl have been measured. Figure 4C illustrates that incubation of 0.6 pM [^{125}I]-TPN-Y1/K12/Q13 with rat Kir1.1 HEK membranes is a time-dependent process that reaches equilibrium in ~5 h. The

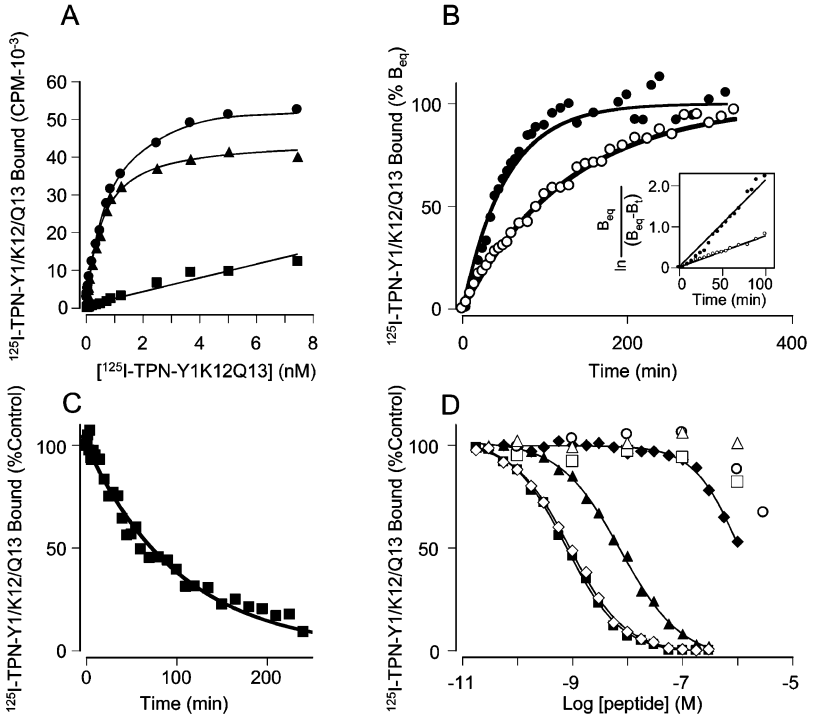

FIGURE 3: Binding of [^{125}I]-TPN-Y1/K12/Q13 to HEK293 cells expressing rat Kir1.1 channels. (A) Saturation studies. HEK293 cells stably transfected with rat Kir1.1 were seeded in 96-well poly-D-lysine-coated plates, at a density of 75 000 cells/well and incubated with increasing concentrations of [^{125}I]-TPN-Y1/K12/Q13 for 8 h at 37 °C. The separation of bound from free ligand was carried out as indicated under the Experimental Procedures. Total binding (●), nonspecific binding determined in the presence of 100 nM TPN-Y1/K12/Q13 (■), and specific binding (▲), defined as the difference between the total and nonspecific binding, are presented. Specific binding was a saturable function of the [^{125}I]-TPN-Y1/K12/Q13 concentration and displayed a K_d of 0.55 nM, Hill coefficient of 1.07, and B_{max} of 91 700 binding sites/cell. (B) Association kinetics. Cells were incubated with 0.07 nM (○) or 0.5 nM (●) [^{125}I]-TPN-Y1/K12/Q13 for indicated amounts of time at 37 °C. Nonspecific binding determined in the presence of 100 nM TPN-Y1/K12/Q13 was time-invariant and has been subtracted from the experimental points. (Inset) Semi-logarithmic representation of the pseudo-first-order association reactions, where B_{eq} and B_t represent ligand bound at equilibrium and time t, respectively, yielded $k_{obs} = 0.76 \times 10^{-2}$ min^{-1} (○) and 2.12×10^{-2} min^{-1} (●), corresponding to k_1 of 2.4×10^7 and 3.3×10^7 M^{-1} min^{-1}, respectively. (C) Dissociation kinetics. After incubation with 0.07 nM [^{125}I]-TPN-Y1/K12/Q13, wells were rinsed and cells were incubated with growth media with or without 100 nM TPN-Y1/K12/Q13 for different periods of time at 37 °C. [^{125}I]-TPN-Y1/K12/Q13 dissociation followed monoexponential kinetics, indicative of a first-order reaction with k_{-1} of 8.7×10^{-3} min^{-1}. (D) Pharmacology. Cells were incubated with 0.07 nM [^{125}I]-TPN-Y1/K12/Q13 in the presence or absence of increasing concentrations of TPN-Q13 (▲), TPN-K12/Q13 (■), TPN-Y1/K12/Q13 (◇), MCDP (◆), α-DTX (△), δ-DTX (○), and Lq2 (□), for 6 h at 37 °C. The inhibition of binding was assessed relative to an untreated control. Specific binding data were fit to a single-site inhibition model, yielding IC_{50} values of 0.77 nM (■), 0.90 nM (◇), and 7.6 nM (▲).

Table 2: Binding of [^{125}I]-TPN-Y1/K12/Q13 to HEK293 Cells Stably Expressing Rat Kir1.1 or Membranes Derived from These Cells[a]

		membranes (pM)	
peptide	cells (nM)	50 mM	100 mM
[^{125}I]-TPN-Y1/K12/Q13	0.57 ± 0.06	1.01 ± 0.12	8.43 ± 0.65
TPN-Q13	6.50 ± 0.90	11.05 ± 1.07	138 ± 40
TPN-K12/Q13	0.54 ± 0.09	0.77 ± 0.21	20 ± 9
TPN-Y1/K12/Q13	0.80 ± 0.06	1.65 ± 0.34	20 ± 6

[a] K_d values were determined from saturation experiments with increasing concentrations of [^{125}I]-TPN-Y1/K12/Q13. Other values represent inhibition constants, K_i values, determined from competition experiments with [^{125}I]-TPN-Y1/K12/Q13 and increasing concentrations of unlabeled peptide. Values represent the mean ± SD of at least three independent determinations.

nonspecific binding component is time-independent and has been subtracted from the experimental data. A semi-logarithmic transformation of the data according to the second-order rate reaction (inset of Figure 4C) yielded a linear dependence, and the slope of this line gives k_1 of 3.1×10^{10} M^{-1} min^{-1}. Dissociation of bound [^{125}I]-TPN-Y1/K12/Q13, initiated either by ligand dilution or by the addition of excess TPN-Y1/K12/Q13, followed a monoexponential decay with a $t_{1/2}$ of ~30 min, corresponding to k_{-1} of 2.3×10^{-2} min^{-1} (Figure 4D). The K_d calculated from these rate constants was 0.74 pM, a value that is similar to that determined under equilibrium binding conditions.

The pharmacology of [^{125}I]-TPN-Y1/K12/Q13 binding to rat Kir1.1 HEK membranes was investigated using different potassium channel modulators. TPN-Q13, TPN-K12/Q13, and TPN-Y1/K12/Q13 inhibited binding of [^{125}I]-TPN-Y1/K12/Q13 (Figure 4E), and K_i values for inhibition are presented in Table 2. TPN peptides are about 10-fold more potent when incubations are carried out in 50 versus 100 mM KCl. Under the latter conditions, MCDP, δ-DTX, Lq2, and ShK inhibit [^{125}I]-TPN-Y1/K12/Q13 binding with K_i values of 16, 45, 810, and 254 nM, respectively. Other peptides, such as apamin, ChTX, IbTX, MgTX, and α-DTX had no effect on [^{125}I]-TPN-Y1/K12/Q13 binding when tested at concentrations of up to 100−1000 nM. Binding of [^{125}I]-TPN-Y1/K12/Q13 was also sensitive to $BaCl_2$ (K_i = 0.26 mM). These data, taken together, indicate that [^{125}I]-TPN-Y1/K12/Q13 binding to rat Kir1.1 HEK membranes occurs to receptor sites that represent Kir1.1 channels and suggest that the peptide−channel interaction could serve as a basis for developing the molecular pharmacology of this channel.

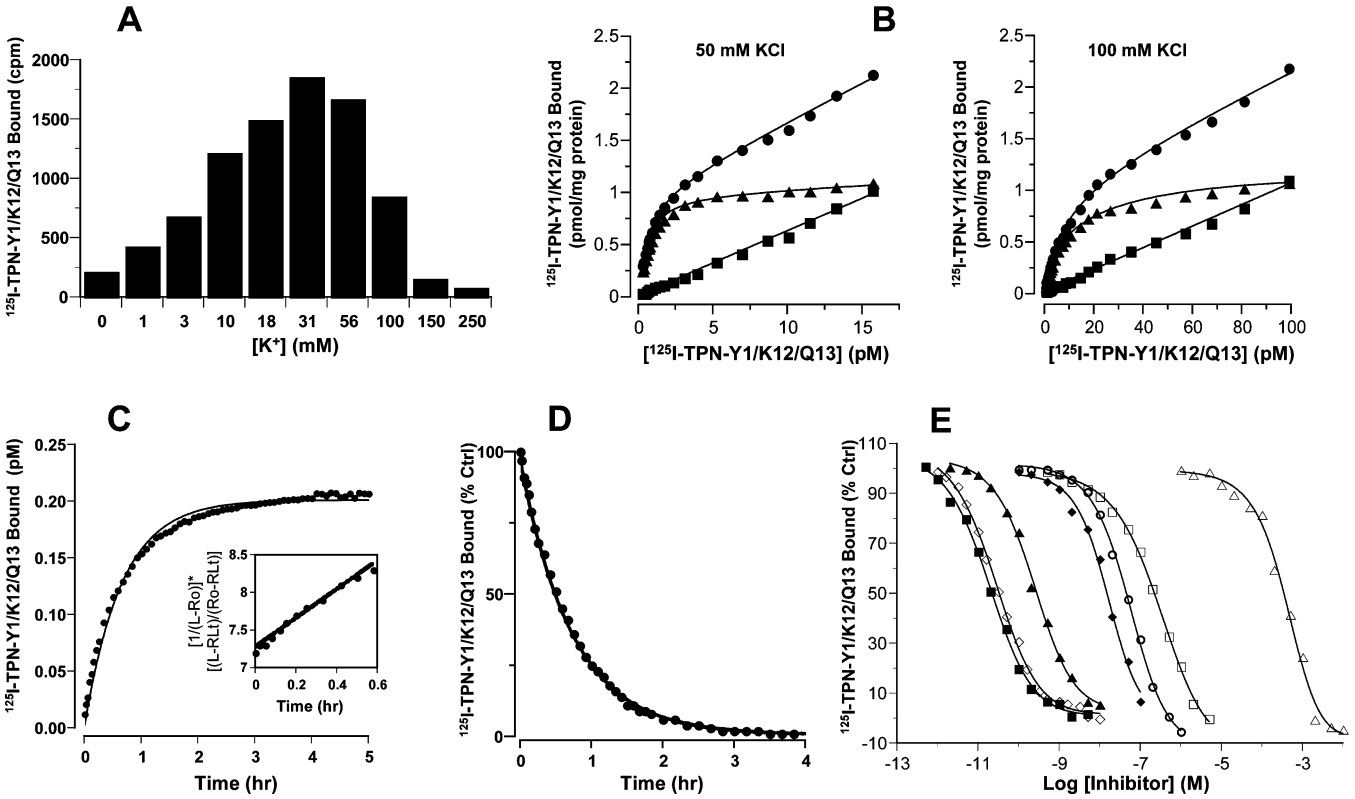

FIGURE 4: Binding of [^{125}I]-TPN-Y1/K12/Q13 to membranes prepared from HEK293 cells expressing rat Kir1.1. (A) Potassium dependence. Membranes prepared from HEK293 cells stably expressing rat Kir1.1 were incubated with 2.5 pM [^{125}I]-TPN-Y1/K12/Q13 in the presence of increasing concentrations of KCl for 6 h at room temperature. Nonspecific binding was determined in the presence of 10 nM TPN-Y1/K12/Q13. The separation of bound from free ligand was achieved as indicated under the Experimental Procedures. (B) Saturation studies. HEK-rKir1.1 membranes were incubated with increasing concentrations of [^{125}I]-TPN-Y1/K12/Q13 in either 50 or 100 mM KCl for 6 h at room temperature. Total binding (●), nonspecific binding defined in the presence of 10 nM TPN-Y1/K12/Q13 (■), and specific binding (▲), defined as the difference between total and nonspecific binding, are presented. Data are fit to a single class of binding sites with K_d values of 0.99 pM (50 mM KCl) and 9.04 pM (100 mM KCl), respectively, and B_{max} of 1.1 pmol/mg of protein. (C) Association kinetics. HEK-rKir1.1 membranes in 50 mM KCl were incubated with 0.6 pM [^{125}I]-TPN-Y1/K12/Q13 for indicated amounts of time at room temperature. Nonspecific binding determined in the presence of 1 nM TPN-Y 1/K12/Q13 was time-invariant and has been subtracted from the experimental points. (Inset) Semi-logarithmic representation of the second-order association reaction, where L_0 is the total ligand concentration, R_0 is the total receptor concentration, and RL is the receptor−ligand complex at a given time *t*. An association rate constant, k_1, of 3.1×10^{10} M^{-1} min^{-1} was determined. (D) Dissociation kinetics. After incubation with 0.6 pM [^{125}I]-TPN-Y1/K12/Q13, dissociation of bound ligand was initiated by the addition of 1 nM TPN-Y1/K12/Q13. [^{125}I]-TPN-Y1/K12/Q13 dissociation followed monoexponential kinetics, indicative of a first-order reaction with k_{-1} of 2.3×10^{-2} min^{-1}. (E) Pharmacology. HEK-rKir1.1 membranes in 100 mM KCl and 20 mM Tris-HCl at pH 7.4 were incubated with 5.4 pM [^{125}I]-TPN-Y1/K12/Q13 in the absence or presence of increasing concentrations of TPN-K12/Q13 (■), TPN-Y1/K12/Q13 (◇), TPN-Q13 (▲), MCDP (◆), δ-dendrotoxin (○), ShK (□), or $BaCl_2$ (△). Specific binding data are fit to a single-site inhibition model, yielding IC_{50} values of 0.019 nM (■), 0.027 nM (◇), 0.2 nM (▲), 15.7 nM (◆), 53.9 nM (○), 296 nM (□), and 0.41 mM (△), respectively.

Inhibition of Human Kir1.1 Channels by TPN-Y1/K12/Q13. During the evaluation of TPN peptides, it was noted that the human Kir1.1 channel was much less sensitive to inhibition by the peptides. A concentration of 300 nM TPN-Y1/K12/Q13 only blocks 53 ± 3% ($n = 4$) of human Kir1.1 (Figure 5D), whereas similar levels of inhibition of rat Kir1.1 channels were observed at ∼1 nM TPN-Y1/K12/Q13. All lines of evidence suggest that the M1−M2 linker region of the channel is solely responsible for the high-affinity interaction of TPN with the channel. A comparison of rat and human sequences in the M1−M2 linker indicate the presence of different amino acids at six positions. Mutagenesis studies have provided evidence that some of these residues play a critical role in the interaction of TPN with rat Kir1.1 (*13*), suggesting that reduced sensitivity of the human channel to the peptide resides within the nature of the M1−M2 linker. In an attempt to understand the molecular basis for the reduced sensitivity of human Kir1.1 to TPN, a number of chimeric molecules were prepared, in which specific residues of the human Kir1.1 M1−M2 linker were exchanged for the equivalent amino acid found in the rat channel (Figure 5A). These constructs were initially analyzed in [^{125}I]-TPN-Y1/K12/Q13-binding experiments to both cells and membrane preparations, followed by electrophysiological recordings, after transient transfection into TsA-201 cells. Substitution of the six nonconserved residues in the human Kir1.1 M1−M2 linker conferred the rat Kir1.1 phenotype with regard to [^{125}I]-TPN-Y1/K12/Q13 binding, strongly supporting the notion that the M1−M2 linker is the only channel determinant for high-affinity TPN interaction with the channel. In addition, a single substitution in human Kir1.1, Phe at Cys148, yields a channel with ∼5−13-fold lower affinity for [^{125}I]-TPN-Y1/K12/Q13 than rat Kir1.1, and the double substitution, Asp116/Phe148, cannot be distinguished in its binding properties from rat Kir1.1. In membranes, binding of [^{125}I]-TPN-Y1/K12/Q13 was not detected to constructs that did not contain the Phe148 substitution, although the presence of the protein was always

A

	M1	M1-M2 linker					M2	Cells (nM)	Membranes (pM)
		113	115	116	118	128	148		
Rat		Y	P	D	R	M	F	1.1 ± 0.4	1.9 ± 0.4
$Human_{wt}$		H	S	A	H	L	C	ND	ND
$Human_{mut1}$		Y	P	D	R	M	F	0.8 ± 0.3	2.8 ± 2.4
$Human_{mut2}$		Y	P	D	R		F	2.2 ± 0.6	3.1 ± 0.1
$Human_{mut3}$							F	5.6 ± 2.4	24.6 ± 1.5
$Human_{mut4}$				D			F	1.3 ± 0.5	1.8 ± 0.8
$Human_{mut5}$		Y	P	D	R	M		ND	ND
$Human_{mut6}$						M		ND	ND
$Human_{mut7}$				D				13.2 ± 3.2	ND
$Human_{mut8}$						M	F	2.8 ± 1.2	ND

B

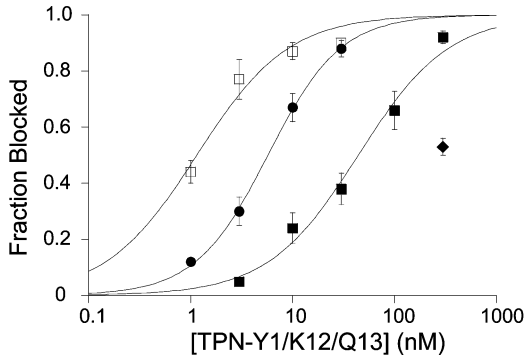

FIGURE 5: Inhibition of hKir1.1 by TPN. (A) Schematic representation of rat and human Kir1.1 in the M1−M2 linker region of the channel showing the six residues that are not conserved between the two species. Numbering refers to rat Kir1.1. Different constructs were prepared in the human Kir1.1 channel background as indicated. Binding of [^{125}I]-TPN-Y1/K12/Q13 to TsA-201 cells transiently transfected with different Kir1.1 constructs or to membranes prepared from these cells was carried out as described under the Experimental Procedures. Specific binding data relative to those of an untreated control were fit to a single-site inhibition model yielding the indicated IC_{50} values. ND = specific binding of [^{125}I]-TPN-Y1/K12/Q13 was not detected for the indicated construct. Values represent the mean ± standard deviation (SD) of two or more independent determinations. (B) Inhibition of hKir1.1 mutants by TPN-Y1/K12/Q13. TsA-201 cells transiently transfected with the hKir1.1 mutants A116D (■) and C148F (●) were analyzed by whole-cell voltage-clamp electrophysiology, as shown in Figure 1 for rat Kir1.1 channels. Data are presented as the average fraction blocked (n = 4), and the solid lines are fits of the Hill equation to the average data with apparent IC_{50} values of 5.7 and 44 nM and slopes of 1.2 and 1.0 for C148F and A116D channels, respectively. Data for the block of wild-type human (◆) and rat Kir1.1 (□) data are shown for a comparison.

confirmed in Western blots using commercially available Kir1.1 polyclonal antibodies (Chemicon, 1:2000; Alomone, 1:2500). Specific immunostaining of three polypeptides was consistently observed after heterologous expression of human Kir1.1. Upon SDS−PAGE in 7% polyacrylamide Tris-acetate gels, these polypeptides display apparent molecular weights of 38, 41, and 54 kDa. The 38 and 41 kDa polypeptides are likely to represent immature and glycosylated human Kir1.1, respectively, whereas the 54 kDa polypeptide could be related to the mono-ubiquitinated form of rat Kir1.1 that has been shown to be present in rat kidney (*25*). In electrophysiological recordings, substitution of Phe at Cys148 yields a channel with an affinity for TPN-Y1-K12/Q13 only 5-fold lower than that of rat Kir1.1 (IC_{50} = 5.7 versus 1.1 nM) (Figure 5B). Thus, Cys148 appears to be responsible for a 50-fold loss in TPN affinity of human Kir1.1. In agreement with the binding experiments, Ala116 also appears to contribute to the binding energy of TPN, because the substitution of Asp at this position enhances the TPN affinity of the human channel ~7-fold. These data, taken together, suggest that the much lower sensitivity of human Kir1.1 to TPN peptides is due to the presence of Ala116 and Cys148 in the M1−M2 linker region of the channel.

DISCUSSION

The results presented in this study concern the development of a high-affinity probe, TPN-Y1/K12/Q13, for characterizing rat Kir1.1 channels and its use to determine the molecular features responsible for diminished sensitivity of human Kir1.1 to the peptide. The radiolabeled peptide, [^{125}I]-TPN-Y1/K12/Q13, represents a novel and quantitative tool with which to study mechanisms that control cell-surface expression of Kir1.1 channels and could also have utility in developing the molecular pharmacology of this channel family.

Although Kir channels play fundamental roles in cell physiology and their structural features are well-understood, the molecular pharmacology of this family of channels

remains undeveloped. The finding that TPN, a small peptide isolated from bee venom, interacts with high affinity with Kir1.1 and Kir3.1/3.4 channels provided the basis for establishing assays with which to search for other Kir modulators (*10*). TPN is not a very stable peptide because its methionine residue at position 13 can undergo air oxidation, resulting in the loss of biological activity. Glutamine substitution at this position leads to a stable and biologically active peptide (*11*). In addition, lysine substitution at histidine 12 removes the pH dependence of the block seen with the parent peptide (*12*). Mechanistic and mutagenesis studies strongly suggest that TPN binds in a 1:1 stoichiometry to the outer vestibule of the channel through the α-helix region, comprised of residues 12−19 (*13*). Because its extended N-terminal region does not participate in channel interaction and appears to project into the extracellular media, it provides a physical location for the incorporation of probes with which to label the peptide.

A convenient way to label peptides consists of the covalent incorporation of ^{125}I into either tyrosine or histidine residues, but because TPN-K12/Q13 does not possess either residue, TPN-Y1/K12/Q13 was prepared as a precursor for high specific activity iodination. Both TPN-Y1/K12/Q13 and [^{127}I]-TPN-Y1/K12/Q13 display biological activities similar to parent peptides as predicted from the lack of contribution of the N terminus to the channel block. Specific, saturable, and reversible binding of [^{125}I]-TPN-Y1/K12/Q13 occurs to cell-surface-expressed rat Kir1.1 channels, as well as to membranes prepared from cells expressing these channels. Having a probe that provides a direct and quantitative measure of those channels present at the cell surface will facilitate studies aimed at understanding mechanisms that control Kir1.1 cell-surface expression. Because of the high open probability of Kir1.1 channels, the regulation of channel activity is predicted to occur through changes in the number of functional channels at the cell surface. Mechanisms such as ubiquitination or phosphorylation of Kir1.1 by the tyrosine kinase Src, PKC, WNK4 kinase, and serum- and glucocorticoid-activated kinase1 (SGK1) have been implicated in regulation of channel activity by retrieving channels from the plasma membrane through a dynamin-dependent endocytotic process that involves clathrin-coated pits (*25*−*28*). Tyrosine phosphorylation of Kir1.1 appears to increase channel internalization in the cortical collecting duct, and this mechanism could account for the response of the kidney to a low potassium diet. On the other hand, phosphorylation of serine 44 in Kir1.1 by PKA and SGK leads to higher cell-surface expression by a mechanism that involves the suppression of a C-terminal ER retention signal. Increased Kir1.1 expression at the cortical collecting duct could account for enhanced potassium excretion after an acute potassium load. Because most of the above studies have involved labor-intensive electrophysiological measurements and/or tagging Kir1.1 or labeling cell-surface proteins with impermeant biotin followed by immunoprecipitation/Western analysis, [^{125}I]-TPN-Y1/K12/Q13 offers a time-saving and quantitative tool without disrupting the system.

Although [^{125}I]-TPN-Y1/K12/Q13 binds to cell-surface channels with similar affinity to that determined for the channel block in electrophysiological measurements, the interaction of the peptide with membranes prepared from the same cells is of higher affinity. For instance, under cell-growth media conditions, K_d for binding to cells is 0.56 nM, but when using membranes, in the presence of 50 mM potassium chloride, K_d values of ∼1 pM were determined. This phenomenon has been previously observed when studying the interaction of other pore-blocking peptides with potassium channels (*17*, *29*), and some of the differences in affinity are likely to reflect the ionic strength effect on TPN binding. In addition, the occupancy of potassium-binding sites in the conduction pore (*24*) or structural changes in the outer vestibule of the channel could be different between cells and membranes and also contribute to the observed differences in potency.

A new finding resulting from this study concerns the observation that human Kir1.1 is ∼300-fold less sensitive to inhibition by TPN peptides than rat Kir1.1. A comparison of the M1−M2 linker amino acid sequences between rat and human Kir1.1 indicates the presence of six nonidentical residues. Some of these residues were found to have significant effects on rat Kir1.1 sensitivity to TPN when mutated to alanine. With the use of chimeras and site-directed mutagenesis, it has been possible to confer TPN sensitivity to human Kir1.1 by substituting two residues in the M1−M2 linker, Ala116 and Cys148, with the corresponding ones of rat Kir1.1. These results are consistent with the proposed mechanism of interaction of TPN with rat Kir1.1 (*13*).

In summary, a high-affinity, high specific activity peptide, [^{125}I]-TPN-Y1/K12/Q13, has been prepared and shown to bind to rat Kir1.1 channels heterologously expressed in HEK293 cells and to membranes derived from these cells. Binding to intact cells allows for an easy and quantitative way of determining cell-surface-expressed channels. The interaction of [^{125}I]-TPN-Y1/K12/Q13 with Kir1.1 channels could be used as an assay for developing the molecular pharmacology of this family of potassium channels.

ACKNOWLEDGMENT

We thank Drs. Magdalena Alonso-Galicia, Euan MacIntyre, and Sophie Roy for discussions and support during the course of this work.

REFERENCES

1. Wickenden, A. (2002) K^+ channels as therapeutic drug targets, *Pharmacol. Ther. 94*, 157−182.
2. Morais Cabral, J. H., Zhou, Y., and MacKinnon, R. (2001) Energetic optimization of ion conduction rate by the K^+ selectivity filter, *Nature 414*, 37−42.
3. Doyle, D. A., Morais Cabral, J., Pfuetzner, R. A., Kuo, A., Gulbis, J. M., Cohen, S. L., Chait, B. T., and MacKinnon, R. (1998) The structure of the potassium channel: Molecular basis of K^+ conduction and selectivity, *Science 280*, 69−77.
4. Matsuda, H., Saigusa, A., and Irisawa, H. (1987) Ohmic conductance through the inwardly rectifying K channel and blocking by internal Mg^{2+}, *Nature 325*, 156−159.
5. Ficker, E., Taglialatela, M., Wible, B. A., Henley, C. M., and Brown, A. M. (1994) Spermine and spermidine as gating molecules for inward rectifier K^+ channels, *Science 266*, 1068−1072.
6. Nishida, M., and MacKinnon, R. (2002) Structural basis of inward rectification: Cytoplasmic pore of the G protein-gated inward rectifier GIRK1 at 1.8 Å resolution, *Cell 111*, 957−965.
7. Kuo, A., Gulbis, J. M., Antcliff, J. F., Rahman, T., Lowe, E. D., Zimmer, J., Cuthbertson, J., Ashcroft, F. M., Ezaki, T., and Doyle, D. A. (2003) Crystal structure of the potassium channel KirBac1.1 in the closed state, *Science 300*, 1922−1926.

8. Dhamoon, A. S., and Jalife, J. (2005) The inward rectifier current (IK1) controls cardiac excitability and is involved in arrhythmogenesis, *Heart Rhythm 2*, 316−324.
9. Ashcroft, F. (2000) *Ion Channels and Disease*, Academic Press, San Diego, CA.
10. Jin, W., and Lu, Z. (1998) A novel high-affinity inhibitor for inward-rectifier K^+ channels, *Biochemistry 37*, 13291−13299.
11. Jin, W., and Lu, Z. (1999) Synthesis of a stable form of tertiapin: A high-affinity inhibitor for inward-rectifier K^+ channels, *Biochemistry 38*, 14286−14293.
12. Ramu, Y., Klem, A. M., and Lu, Z. (2001) Titration of tertiapin-Q inhibition of ROMK1 channels by extracellular protons, *Biochemistry 40*, 3601−3605.
13. Jin, W., Klem, A. M., Lewis, J. H., and Lu, Z. (1999) Mechanisms of inward-rectifier K^+ channel inhibition by tertiapin-Q, *Biochemistry 38*, 14294−14301.
14. Suarez-Kurtz, G., Vianna-Jorge, R., Pereira, B. F., Garcia, M. L., and Kaczorowski, G. J. (1999) Peptidyl inhibitors of shaker-type Kv1 channels elicit twitches in guinea pig ileum by blocking Kv1.1 at enteric nervous system and enhancing acetylcholine release, *J. Pharmacol. Exp. Ther. 289*, 1517−1522.
15. Middleton, R. E., Sanchez, M., Linde, A. R., Bugianesi, R. M., Dai, G., Felix, J. P., Koprak, S. L., Staruch, M. J., Bruguera, M., Cox, R., Ghosh, A., Hwang, J., Jones, S., Kohler, M., Slaughter, R. S., McManus, O. B., Kaczorowski, G. J., and Garcia, M. L. (2003) Substitution of a single residue in *Stichodactyla helianthus* peptide, ShK-Dap22, reveals a novel pharmacological profile, *Biochemistry 42*, 13698−13707.
16. Hanner, M., Green, B., Gao, Y. D., Schmalhofer, W. A., Matyskiela, M., Durand, D. J., Felix, J. P., Linde, A. R., Bordallo, C., Kaczorowski, G. J., Kohler, M., and Garcia, M. L. (2001) Binding of correolide to the Kv1.3 potassium channel: Characterization of the binding domain by site-directed mutagenesis, *Biochemistry 40*, 11687−11697.
17. Knaus, H. G., Koch, R. O., Eberhart, A., Kaczorowski, G. J., Garcia, M. L., and Slaughter, R. S. (1995) [^{125}I]margatoxin, an extraordinarily high affinity ligand for voltage-gated potassium channels in mammalian brain, *Biochemistry 34*, 13627−13634.
18. Priest, B. T., Garcia, M. L., Middleton, R. E., Brochu, R. M., Clark, S., Dai, G., Dick, I. E., Felix, J. P., Liu, C. J., Reiseter, B. S., Schmalhofer, W. A., Shao, P. P., Tang, Y. S., Chou, M. Z., Kohler, M. G., Smith, M. M., Warren, V. A., Williams, B. S., Cohen, C. J., Martin, W. J., Meinke, P. T., Parsons, W. H., Wafford, K. A., and Kaczorowski, G. J. (2004) A disubstituted succinamide is a potent sodium channel blocker with efficacy in a rat pain model, *Biochemistry 43*, 9866−9876.
19. Hamill, O. P., Marty, A., Neher, E., Sakmann, B., and Sigworth, F. J. (1981) Improved patch-clamp techniques for high-resolution current recording from cells and cell-free membrane patches, *Pflugers Arch. 391*, 85−100.
20. Lu, Z., and MacKinnon, R. (1997) Purification, characterization, and synthesis of an inward-rectifier K^+ channel inhibitor from scorpion venom, *Biochemistry 36*, 6936−6940.
21. Imredy, J. P., Chen, C., and MacKinnon, R. (1998) A snake toxin inhibitor of inward rectifier potassium channel ROMK1, *Biochemistry 37*, 14867−14874.
22. Vazquez, J., Feigenbaum, P., King, V. F., Kaczorowski, G. J., and Garcia, M. L. (1990) Characterization of high affinity binding sites for charybdotoxin in synaptic plasma membranes from rat brain. Evidence for a direct association with an inactivating, voltage-dependent, potassium channel, *J. Biol. Chem. 265*, 15564−15571.
23. Helms, L. M., Felix, J. P., Bugianesi, R. M., Garcia, M. L., Stevens, S., Leonard, R. J., Knaus, H. G., Koch, R., Wanner, S. G., Kaczorowski, G. J., and Slaughter, R. S. (1997) Margatoxin binds to a homomultimer of Kv1.3 channels in Jurkat cells. Comparison with Kv1.3 expressed in CHO cells, *Biochemistry 36*, 3737−3744.
24. Zhou, Y., and MacKinnon, R. (2003) The occupancy of ions in the K^+ selectivity filter: Charge balance and coupling of ion binding to a protein conformational change underlie high conduction rates, *J. Mol. Biol. 333*, 965−975.
25. Lin, D. H., Sterling, H., Wang, Z., Babilonia, E., Yang, B., Dong, K., Hebert, S. C., Giebisch, G., and Wang, W. H. (2005) ROMK1 channel activity is regulated by monoubiquitination, *Proc. Natl. Acad. Sci. U.S.A. 102*, 4306−4311.
26. Lin, D. H., Sterling, H., Yang, B., Hebert, S. C., Giebisch, G., and Wang, W. H. (2004) Protein tyrosine kinase is expressed and regulates ROMK1 location in the cortical collecting duct, *Am. J. Physiol. Renal Physiol. 286*, F881−F892.
27. O'Connell, A. D., Leng, Q., Dong, K., MacGregor, G. G., Giebisch, G., and Hebert, S. C. (2005) Phosphorylation-regulated endoplasmic reticulum retention signal in the renal outer-medullary K^+ channel (ROMK), *Proc. Natl. Acad. Sci. U.S.A. 102*, 9954−9959.
28. Yoo, D., Fang, L., Mason, A., Kim, B.-Y., and Welling, P. A. (2005) A phosphorylation-dependent export structure in ROMK (Kir 1.1) channel overrides an endoplasmic reticulum localization signal, *J. Biol. Chem. 280*, 35281−35289.
29. Vazquez, J., Feigenbaum, P., Katz, G., King, V. F., Reuben, J. P., Roy Contancin, L., Slaughter, R. S., Kaczorowski, G. J., and Garcia, M. L. (1989) Characterization of high affinity binding sites for charybdotoxin in sarcolemmal membranes from bovine aortic smooth muscle. Evidence for a direct association with the high conductance calcium-activated potassium channel, *J. Biol. Chem. 264*, 20902−20909.

BI060509S